



Technical Note

The influence of PV coverage ratio on thermal and electrical performance of photovoltaic-Trombe wall

Bin Jiang^{a,*}, Jie Ji^b, Hua Yi^b^a*Faculty of Urban Construction and Environmental Engineering, Chongqing University, Chongqing 400045, China*^b*Department of Thermal Science and Energy Engineering, University of Science and Technology of China, Hefei 230026, China*

Received 6 September 2007; accepted 3 February 2008

Abstract

This paper presents a novel photovoltaic-Trombe wall (PV-TW). Based on the actual measured weather data in Hefei, a detailed simulation model for PV-TW is presented. The simulation results show that as the coverage ratio increases, the electrical yield and the total efficiency of PV-TW increases, but the indoor temperature and the thermal efficiency of PV-TW decreases. The maximum indoor air temperature difference, corresponding to the lowest and the highest coverage ratio, can reach to 6.8 °C above. In addition, as the coverage ratio increases, the electrical efficiency of photovoltaic cell decreases, but the influence of coverage ratio on electrical efficiency is slight, less than 0.5%.

© 2008 Elsevier Ltd. All rights reserved.

Keywords: Photovoltaic-Trombe wall; Coverage ratio; Electrical yield; Heat gain through the PV-TW; Thermal efficiency; Total efficiency**1. Introduction**

Trombe wall, as an effective passive solar building facade system, is a south-facing concrete or masonry wall blackened and covered on the exterior by glazing. The massive wall serves to collect and storage solar energy. The stored energy is transferred to the inside building for winter heating or facilitates room air movement for summer cooling. Its applications are simple and economical, and are suitable for locations at a wide range of latitudes. In the last decade, photovoltaic (PV) cell has been under active technological developments [1]. Its market growth has been at an exponential rate. Nevertheless, presently a commercial PV cell still converts not more than 15% of the incoming solar energy to electrical energy. The remaining portion is either reflected or absorbed as heat energy. Without an effective means of dissipating this absorbed energy, the heat accumulation will cause substantial elevation of the working temperature of the PV cells. This progressively reduces the cell electrical efficiency and lowers the electricity yield even

at a higher level of available solar radiation. Integrating PV panels into a building facade represents a significant step forward in the application of his relatively new technology. Such a facade serves not only as a renewable source of electricity, but also as a source of heat for building heating and cooling. Various authors have modeled the ventilated PV facade by evaluation of energy inputs and outputs through radiation, convection, conduction and electrical yield, [2,3]. Much thermal analysis based on steady state energy balance and more complex simulation programs using computational fluid dynamic (CFD) approach have been developed [4–7]. Based on dynamic general finite element thermal model and TRNSYS program, a complete thermal building model incorporating a ventilated PV facade and solar air collectors has been assembled [8]. However, the combination of PV cells and Trombe wall has not been researched recently.

In this paper, a novel photovoltaic-Trombe wall (PV-TW) is proposed. Based on the actual measured weather data in Hefei, a detailed simulation model for PV-TW is presented. With the simulation program, the electrical performance of PV cells and the thermal performance of PV-TW in different coverage ratio have been investigated.

*Corresponding author. Tel./fax: +86 816 6089957.

E-mail address: jiangbin@swust.edu.cn (B. Jiang).

Nomenclature

$A_{\text{glass}}, A_{\text{pv}}$ area of PV-glazing and photovoltaic cells, respectively (m^2)
 $C_{\text{in}}, C_{\text{out}}$ loss coefficients at top vent and bottom vent, respectively
 C_f friction factor along the air duct
 C_p, C_w, C_g specific heat capacity of air, wall and glass, respectively (J/kg K)
 d air duct hydraulic diameter
 D, D_w depth of air duct, the thickness of the massive wall (m)
 E electrical yield of photovoltaic cells (kWh)
 g gravitational acceleration, $g = 9.80665 \text{ (m/s}^2\text{)}$
 G total solar radiation (W/m^2)
 $h_{\text{co}}, h_{\text{ci}}$ convection heat transfer coefficients on the outside surface and inside surface of PV-glazing ($\text{W/m}^2 \text{K}$)
 $h_{\text{ro}}, h_{\text{ri}}$ radiation heat transfer coefficients on out side surface and inside surface of PV-glazing ($\text{W/m}^2 \text{K}$)
 $h_{\text{wo}}, h_{\text{wi}}$ convection heat transfer coefficients on the outside surface and the inside surface of massive wall, respectively ($\text{W/m}^2 \text{K}$)
 h_{rwo} radiation heat transfer coefficient on the outside surface of massive wall ($\text{W/m}^2 \text{K}$)
 h_{nrwo} radiation heat transfer coefficient on the outside surface of normal wall ($\text{W/m}^2 \text{K}$)
 h_{nwi} convection heat transfer coefficient on the inside surface of normal wall ($\text{W/m}^2 \text{K}$)
 L height of PV-TW (m)
 L_{room} depth of room (m)
 \dot{m} ventilated mass flow (kg/s)
 Q_k heat transmitted to the interior of room through the massive wall of PV-TW (kWh)

Q_c thermal-circulation heat gain of PV-TW (kWh)
 R_{Trombe} ratio between the area of PV-Trombe wall and the southern wall
 T_p, T_e, T_a temperatures of PV-glazing, ambient, the air in the duct, respectively ($^\circ\text{C}$)
 $T_{\text{wo}}, T_{\text{wi}}$ temperatures of outside and inside surface of massive wall ($^\circ\text{C}$)
 $T_{\text{nwo}}, T_{\text{nwi}}$ temperatures of outside and inside surface of normal wall ($^\circ\text{C}$)
 $T_{\text{out}}, T_{\text{in}}$ temperatures of top vent and bottom vent ($^\circ\text{C}$)
 T_r indoor temperature ($^\circ\text{C}$)
 V_a velocity of the air flow in the duct (m/s)
 w width of PV-TW (m)
 X calculation height (m)

Greek symbols

$\alpha, \alpha_{\text{nwall}}, \alpha_{\text{wall}}$ absorptivity of the PV-glazing, the normal wall, massive wall, respectively
 τ transmittance of glass
 δ thickness of the glass
 η_0 electrical efficiency of photovoltaic cells at standard conditions
 η_e electrical efficiency of photovoltaic cells
 $\eta_{\text{e,sys}}$ electrical efficiency of PV-TW
 η_{th} thermal efficiency of PV-TW
 η_{power} normal fuel electric plant efficiency
 η_{total} total efficiency of PV-TW
 ρ, ρ_g, ρ_w density of the air, glass, wall, respectively (kg/m^3)
 ξ_1, ξ_2, ξ_3 emissivity factors
 $\lambda_a, \lambda_g, \lambda_w$ thermal conductivity of air, glass, wall, respectively (W/mK)
 σ Stefan–Boltzman constant, $5.67 \times 10^{-8} \text{ W/m}^2 \text{K}^4$

2. Theoretical analysis

The PV-TW is the original Trombe wall with PV-glazing, which distributed with small square PV cells showed in Fig. 1(a). The coverage ratio of PV-glazing is defined as

$$\varepsilon = \frac{A_{\text{pv}}}{A_{\text{glass}}}, \tag{1}$$

where the A_{pv} is the area of PV cells, A_{glass} is the area of PV-glazing.

2.1. The energy balance of PV-glazing

As the PV cell is flimsy and be well affixed to the back of glass, so the distribution of temperature in horizontal direction can be assumed uniform. But because the different absorptivity of elements with and without PV cells, the temperatures of elements with and without PV

cells are quite different, hence the temperature distribution of PV-glazing can be considered as two-dimensional, in vertical direction and horizontal direction. This is quite different from the Refs. [9–13] which the temperature distribution of glazing is considered as one-dimensional, in vertical direction. For the convenience of calculation, the temperature of every small square PV cell can be considered uniform. As can be seen in Fig. 1(a), the PV-glazing is subdivided into a grid of $m \times n$ control volumes, along the boundary of PV cell. As the PV cell is flimsy, the heat capacity is neglectable. The energy balance of PV-glazing is as follows:

$$\rho_g c_g \frac{\partial T_p}{\partial t} = \frac{\partial}{\partial x} \left(\lambda_g \frac{\partial T_p}{\partial x} \right) + \frac{\partial}{\partial z} \left(\lambda_g \frac{\partial T_p}{\partial z} \right) + b, \tag{2}$$

where $b = (S_c + S_p T_p) / \delta$.

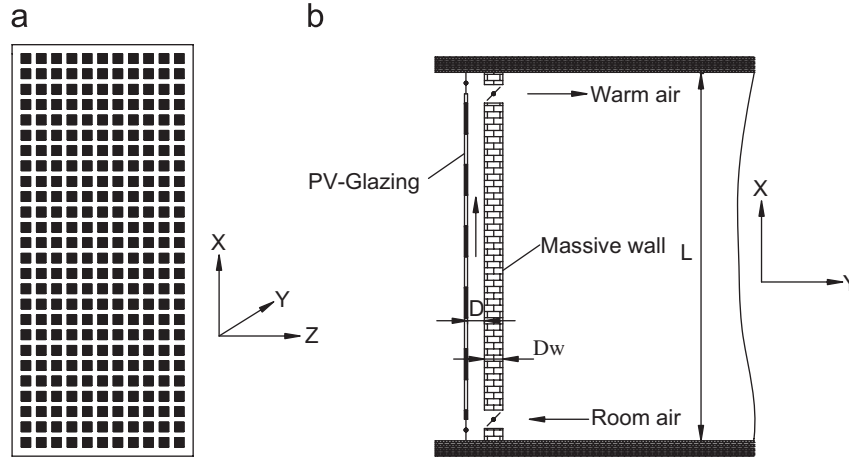


Fig. 1. Schematic diagram of: (a) PV-glazing and (b) PV-TW.

- The element with PV cells

$$S_c = [\alpha\tau + (1 - \tau)]G - E + h_{co}T_e + \xi_1 h_{ro}T_e + h_{ci}T_a + \xi_2 h_{ri}T_{wo}, \quad (3)$$

$$S_p = -(h_{co} + \xi_1 h_{ro} + h_{ci} + \xi_2 h_{ri}). \quad (4)$$

- The element without PV cells

$$S_c = G(1 - \tau) + h_{co}T_e + \xi_1 h_{ro}T_e + h_{ci}T_a + \xi_2 h_{ri}T_{wo}, \quad (5)$$

$$S_p = -(h_{co} + \xi_1 h_{ro} + h_{ci} + \xi_2 h_{ri}), \quad (6)$$

where ρ_g , c_g , λ_g , δ are the density of glass, heat capacity of glass, thermal conductivity of glass and thickness of the glass, respectively; α is the absorptivity of PV cell; τ is the transmittance of PV cell; G is the total solar radiation captured by PV-glazing; T_p , T_e , T_a and T_{wo} are the temperatures of PV-glazing, ambient air, the air in the duct and the outside surface of massive wall, respectively; h_{co} , h_{ci} are the convection heat transfer coefficients on the outside surface of PV-glazing and inside surface of PV-glazing; ξ_1 , ξ_2 are the emissivity factors.

E is the electric power output generated by the PV-glazing [14]

$$E = G\eta_0[1 - 0.0045(T_p - 298.15)], \quad (7)$$

where η_0 is the electrical efficiency at standard conditions, 14%.

2.2. Heat transfer coefficient and emissivity factor

2.2.1. Convection heat transfer coefficient

The average convection heat transfer coefficient due to the wind on the outside surface of PV-glazing is as follows [15]:

$$h_{co} = 5.7 + 3.8V. \quad (8)$$

The convection heat transfer coefficient on the inside surface of PV-glazing is calculated from

$$h_{ci} = \frac{Nu_x \lambda_a}{X}, \quad (9)$$

where V is average wind velocity over the PV-glazing, λ_a is the thermal conductivity of air, Nu_x is the local Nusselt number, X is calculation height.

According to the Ref. [13],

$$Nu_x = 0.12(G_{rx} \times P_r)^{1/3}, \quad (10)$$

$$G_{rx} = g\beta(T_p - T_a)X^3/v^2, \quad (11)$$

$$P_r = v/\alpha_a, \quad (12)$$

$$\alpha_a = \lambda_a/\rho C_p, \quad (13)$$

where ρ is the density of air, C_p is the specific heat capacity of air, v is the kinematic viscosity of air, α_a is the thermal diffusivity of air.

2.2.2. Radiation heat transfer coefficient

The radiation heat transfer coefficient on outside surface of PV-glazing can be written as

$$h_{ro} = \sigma(T_p^2 + T_e^2)(T_p + T_e). \quad (14)$$

The radiation heat transfer coefficient on inside surface of PV-glazing can be written as

$$h_{ri} = \sigma(T_p^2 + T_{wo}^2)(T_p + T_{wo}), \quad (15)$$

where σ is the Stefan–Boltzman constant, $5.67 \times 10^{-8} \text{ W/m}^2 \text{ K}^4$.

2.2.3. The emissivity factors on the both sides of PV-glazing

The emissivity factors ξ_1 , ξ_2 are calculated from

$$\frac{1}{\xi_1} = \frac{1}{\epsilon_o} + \frac{1}{\epsilon_e} - 1, \quad (16)$$

$$\frac{1}{\xi_2} = \frac{1}{\epsilon_i} + \frac{1}{\epsilon_{wo}} - 1, \quad (17)$$

where ε_i , ε_o , ε_{wo} , ε_e are the emissivities of inside surface of PV-glazing, outside surface of PV-glazing, outside surface of massive wall and environment, respectively.

2.3. The energy balance of air in the air duct

The air temperature in the air duct varies along the vertical direction, can be determined from an energy balance on a differential unit of air in the air duct perpendicular to the flow direction. The energy balance is as follows:

$$\rho DC_p \frac{dT_a}{dt} = h_{ci}(T_p - T_a) + h_{wo}(T_{wo} - T_a) - \rho V_a DC_p \frac{dT_a}{dX}, \quad (18)$$

where D is the depth of the air duct, w is the width of PV-TW, C_p is the specific heat capacity of air, ρ is the density of air, T_{wo} is the temperature of the outside surface of massive wall, V_a is the velocity of the air flow in the duct.

The air velocity V_a can be calculated from

$$V_a = \sqrt{\frac{0.5 \times g \bar{\beta} (T_{out} - T_{in}) L}{C_f \frac{L}{d} + \frac{C_{in} A^2}{A_{in}^2} + \frac{C_{out} A^2}{A_{out}^2}}}, \quad (19)$$

$$\bar{\beta} = \frac{1}{\bar{T}} = \left(\frac{T_{in} + T_{out}}{2} \right)^{-1} = \frac{2}{T_{in} + T_{out}}, \quad (20)$$

where L is the height of PV-TW, d is the air duct hydraulic diameter, i.e. $d = 2(w + D)$, A is section area of air duct in the height direction, A_{out} , A_{in} are the area of top vent and bottom vent, T_{out} , T_{in} are temperatures of top vent and bottom vent, respectively, C_f , C_{out} , C_{in} are the friction factors along the air duct, loss coefficient at the top vent, loss coefficient at bottom vent, respectively, $C_f = 0.3 \times 1.368 \times G_{rx}^{0.084}$, $C_{out} = 0.3$, $C_{in} = 0.25$.

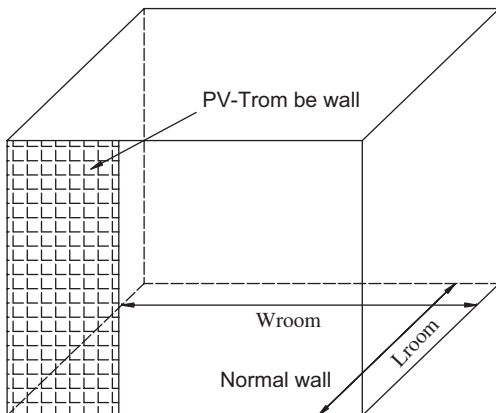


Fig. 2. Schematic diagram of the environmental chamber.

2.4. Heat transfer across the massive wall

As showed in Fig. 2, the southern face of the environmental chamber is composed of the PV-TW and normal wall. It is assumed that the heat transfer is one-dimensional.

For PV-TW, the unsteady heat conduction equation is

$$\frac{\partial T}{\partial t} = \frac{\lambda_w}{\rho_w C_w} \frac{\partial^2 T}{\partial Y^2}, \quad (21)$$

$$-\lambda_w \left(\frac{\partial T}{\partial Y} \right)_{y=0} = h_{wo}(T_{wo} - T_a) + \xi_3 h_{rwo}(T_{wo} - T_p) + G \alpha_{wall} \tau (1 - \varepsilon),$$

$$-\lambda_w \left(\frac{\partial T}{\partial Y} \right)_{y=D_w} = h_{wi}(T_{wi} - \bar{T}_r),$$

$$T_{\tau=0} = T|_0(Y),$$

where ρ_w is the density of the massive wall, C_w is the specific heat capacity of the massive wall, λ_w is the thermal conductivity of the massive wall, α_{wall} is the absorptivity on the outside surface of massive wall, \bar{T}_r is the mean indoor temperature, h_{wo} , h_{rwo} are the convection heat transfer coefficient and radiation heat transfer coefficient on the outside surface of massive wall, respectively, h_{rwo} is the same as h_{ri} , h_{wi} is the convection heat transfer coefficient on the inside surface of massive wall, the emissivity factor ξ_3 is the same as ξ_2 .

For the normal wall, the unsteady conduction equation is as follows:

$$\frac{\partial T}{\partial t} = \frac{\lambda_w}{\rho_w C_w} \frac{\partial^2 T}{\partial Y^2}, \quad (22)$$

$$-\lambda_w \left(\frac{\partial T}{\partial Y} \right)_{y=0} = h_{nwo}(T_{nwo} - T_e) + \xi_1 h_{nrwo}(T_{nwo} - T_e) + G \alpha_{nwall},$$

$$-\lambda_w \left(\frac{\partial T}{\partial Y} \right)_{y=D_w} = h_{nwi}(T_{nwi} - \bar{T}_r),$$

where T_{nwo} , T_{nwi} are the temperatures of outside and inside surface of normal wall, h_{nwo} , h_{nrwo} are convection heat transfer coefficient and radiation heat transfer coefficient on the outside surface of normal wall, h_{nwi} is the convection heat transfer coefficient on the inside surface of normal wall, α_{nwall} is the absorptivity of normal wall.

2.5. The heat transfer process of the air in the room

Comparing with other three normal walls (eastern wall, western wall and northern wall), the heat transfer process of southern wall is more important in the present study, thereby the heat transfer process of southern wall is only

considered. The heat transfer equation is as follows:

$$\rho C_p L_{\text{room}} \frac{dT_r}{dt} = R_{\text{Trombe}} \times h_{\text{wi}}(T_{\text{wi}} - T_r) + (1 - R_{\text{Trombe}}) \times h_{\text{nwi}}(T_{\text{nwi}} - T_r) - \frac{\dot{m} C_p}{w_{\text{room}}} \frac{dT_r}{dX}, \quad (23)$$

where w_{room} , L_{room} are the width and depth of the room, \dot{m} is the mass flow entrance into the room from the top vent, R_{Trombe} is the ratio between the area of PV-Trombe wall and the southern wall.

3. The numerical study

In order to predict the improvement of PV-TW on the indoor thermal environment and electrical performance of PV cells, a simulation program is written in FORTRAN by authors. Based on the actual measured weather data in Hefei, from January 1 to 3, 2005 (in winter), the electrical performance of PV cells, temperature distribution and heat gain through PV-TW are discussed. The following parameters were employed in the simulation:

The structure parameters of PV-TW: The width of PV-TW, $w = 0.84$ m; the height of PV-TW, $L = 2.66$ m; the depth of air duct, $D = 0.13$ m; the area of vent, $A = 0.04$ m²; the width of the room, $w_{\text{room}} = 3.00$ m; the height of room, $L = 2.66$ m; and the depth of room, $L_{\text{room}} = 3.00$ m.

The parameters of air: The density of air, $\rho = 1.18$ kg/m³; the specific heat capacity of air, $C_p = 1000$ J/kg K; the thermal conductivity of air, $\lambda_a = 0.026$ W/mK; the kinematic viscosity of air, $\nu = 1.58 \times 10^{-5}$ m²/s.

The parameters of PV-glazing: The density of the glass, $\rho_g = 2515$ kg/m³; the specific heat capacity of the glass, $C_g = 810$ J/kg K; the thermal conductivity of the glass, $\lambda_g = 1.4$ W/mK; the thickness of the glass, $\delta = 3$ mm; the transmittance of glass, $\tau = 0.9$; the absorptivity of the PV-glazing, $\alpha = 0.9$; the emissivity of the PV-glazing is 0.9.

The parameters of the normal wall: The thickness of the normal wall, $D_w = 240$ mm; the density of the normal wall, $\rho_w = 1800$ kg/m³; the specific heat capacity of the normal wall, $C_w = 840$ J/kg K; the thermal conductivity of the normal wall, $\lambda_w = 0.814$ W/mK; the absorptivity of the normal wall, $\alpha_{\text{nwall}} = 0.72$; the emissivity of the normal wall is 0.9.

The parameters of the massive wall in the PV-TW: The absorptivity of the massive wall in the PV-TW, $\alpha_{\text{wall}} = 0.9$ and the top vent and the bottom vent were opened at 10:00, and were closed at 16:00. The interval is 5 s. The calculation was started at 1:00.

3.1. The temperature difference between the elements with and without PV cells

For the different absorptivity between the elements with and without PV cells, the temperatures of these two elements are quite different. Hence the temperatures of the elements with and without PV cells were calculated

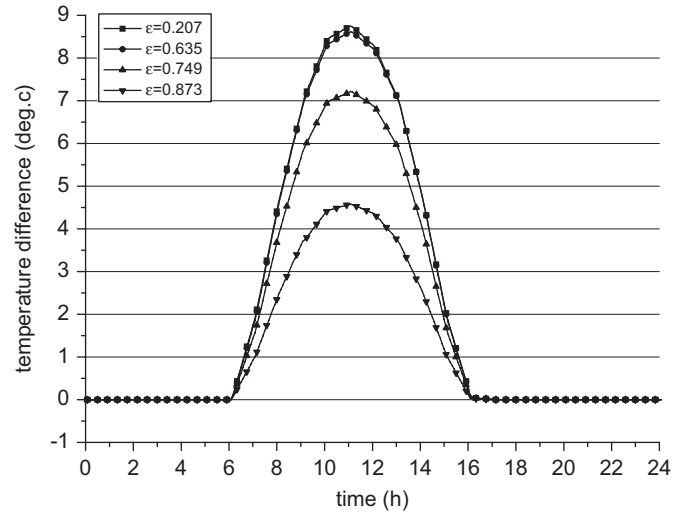


Fig. 3. The temperature difference between the elements with and without photovoltaic cells, in different coverage ratio.

separately. Fig. 3 is the temperature difference between the elements with and without PV cells, in different coverage ratio. When the coverage ratio is of low value, the maximum temperature difference between the elements with and without PV cells can reach to 8.5 °C above. As the coverage ratio increases, the temperature difference decreases.

3.2. The electrical efficiency of PV cells

The temperature of PV cell plays an important role in the electrical efficiency. The electrical efficiency of PV cell, which is the function of the temperature of PV cell, is given by [14]

$$\eta_e = \eta_0 [1 - 0.0045(T_p - 298.15)]. \quad (24)$$

As can be seen from the Eq. (24), as the temperature of PV cell increases, the electrical efficiency reduces. In the present study, when the coverage ratio increases, the solar radiation transmitted to the air duct decreases, thereby the air flow driven by the air thermo-circulation becomes even slow, and the heat taken away by the air thermo-circulation reduces, as a result, the temperature of PV cell increases and the electrical efficiency reduces. Fig. 4 is the temperature of PV cell in different coverage ratio, and Fig. 5 is the electrical efficiency in different coverage ratio. Because the weather data employed in the simulation program is in winter, (from January 1 to 3) as a result, the temperature of PV cell is lower than 25 °C, so from the Eq. (24) one can see that the electrical efficiency is higher than η_0 , which is showed in Fig. 5. Fig. 5 has already showed that, after the vent was closed at 16:00 pm, the thermal-circulation in the duct is cut down, thereby the temperature of PV cell increases which makes the electrical efficiency decrease. Meanwhile, it also can be seen that in winter the influence of coverage ratio on electrical efficiency is slight, less than 0.5%.

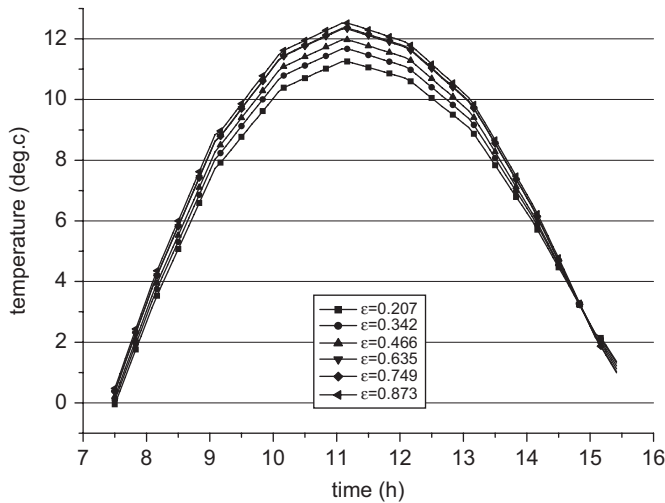


Fig. 4. The temperatures of photovoltaic cells in different ratio of coverage, from 7:00 to 16:00 in one day.

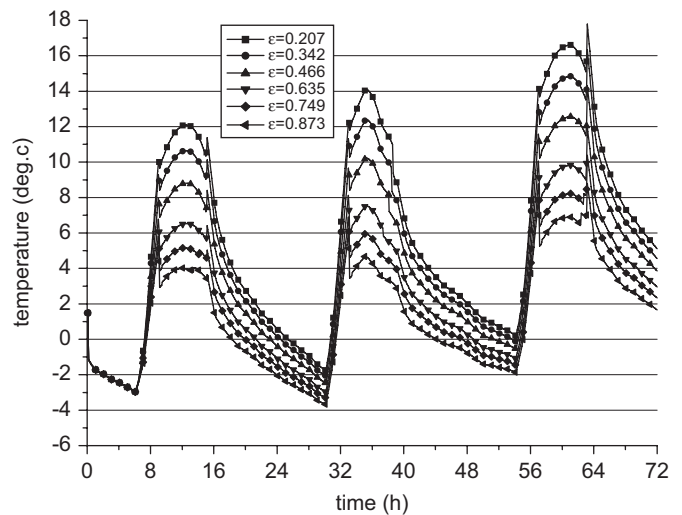


Fig. 6. The air temperature in the duct in different coverage ratio.

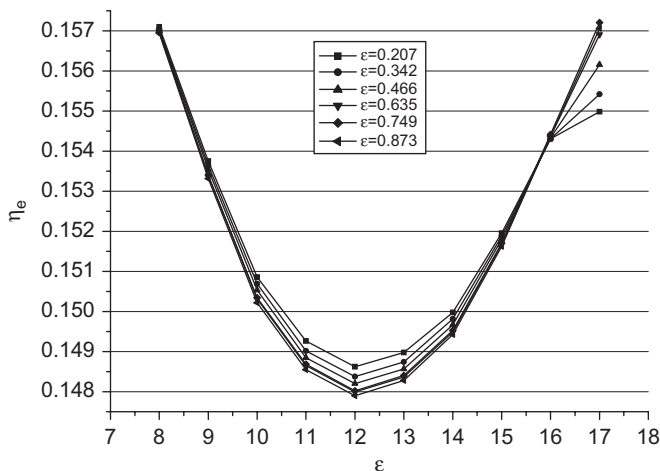


Fig. 5. The electrical efficiency in different ratio of coverage, from 7:00 to 16:00 in one day.

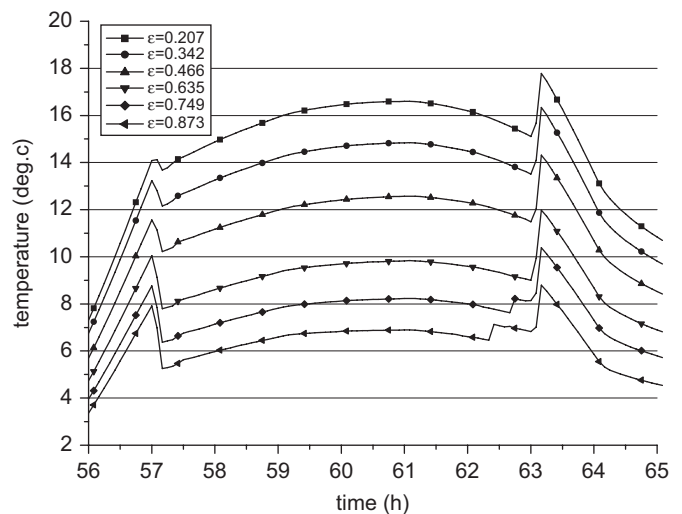


Fig. 7. The enlarged view of Fig. 6, from the 56th hour to the 65th hour.

3.3. The air temperature in the air duct

Fig. 6 is the air temperature in the air duct. One can see that as the coverage ratio increases, the air temperature in the air duct decreases. The reason is that when the coverage ratio increases, the solar radiation transmitted to the air duct decreases, so the heat gain which the air in the duct gets from the blackened surface of the massive wall and the inside surface of PV-glazing reduces. The fluctuations of the temperature at 10:00 am and 16:00 pm (can be seen clearly in Fig. 7) in the day time are because the opening and the closing of the vents.

3.4. The indoor air temperature

Fig. 8 shows the indoor air temperature in different coverage ratio. One can see that as the coverage ratio increases, the air temperature decreases. Because the air in

the duct and the room is continuous, so the reason for the phenomena is same as that in the duct. The unnecessary details will not be given here. The maximum temperature difference, corresponding to the lowest and the highest coverage ratio, can reach to 6.8 °C above. Therefore, in order to get a comfortable thermal environment, an appropriate coverage ratio should be chosen.

3.5. The electrical yield and the heat gain through PV-TW

It is known to all that the larger area of the PV cells is, the more electricity will be yielded, which is showed in Fig. 9. Part of the solar radiation captured by the PV-glazing is converted into electricity, and the rest is converted into thermal energy which is taken away by the air in the duct. The solar radiation captured by the massive wall of PV-TW is transmitted to the interior of the room simultaneously by the process of radiation, convection and thermo-circulation.

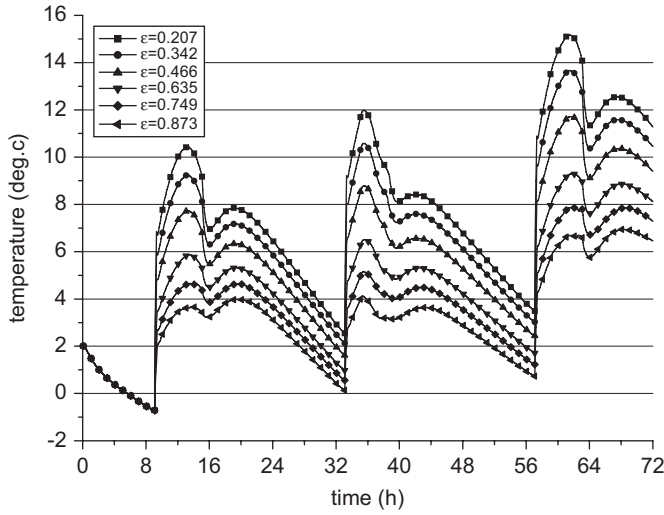


Fig. 8. The indoor air temperature in different coverage ratio.

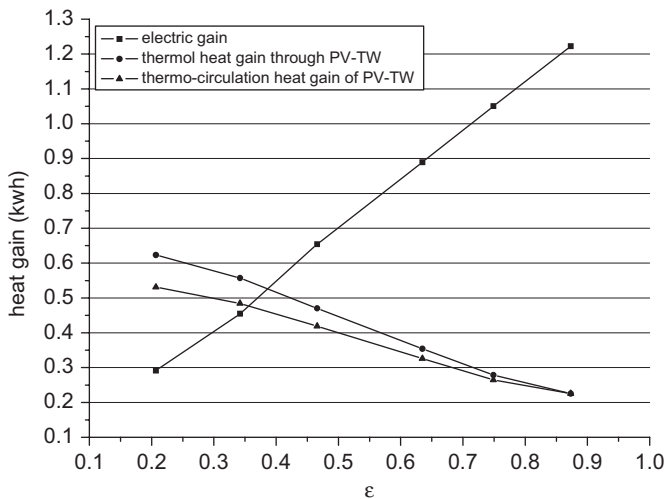


Fig. 9. The electrical yield, thermal heat gain through PV-TW and thermo-circulation heat gain of PV-TW, in different coverage ratio.

However, as the coverage ratio increases, the solar radiation captured by the massive wall becomes even less. Therefore, the heat transmitted to the interior of the room by the massive wall reduces. This becomes the worst when the coverage ratio reaches to 0.87. The contribution of the massive wall to the interior of room becomes heat loss, instead of heat gain. It can be seen clearly in Fig. 9. The thermal heat gain through PV-TW is calculated from

$$Q_{th} = Q_c + Q_k, \quad (25)$$

where Q_c is the thermal-circulation heat gain of PV-TW, Q_k is the heat transmitted to the interior of room through the massive wall of PV-TW.

3.6. The efficiency of the PV-TW

Compare with the thermal energy, the electricity is of high quality. Therefore, when the total efficiency of PV-

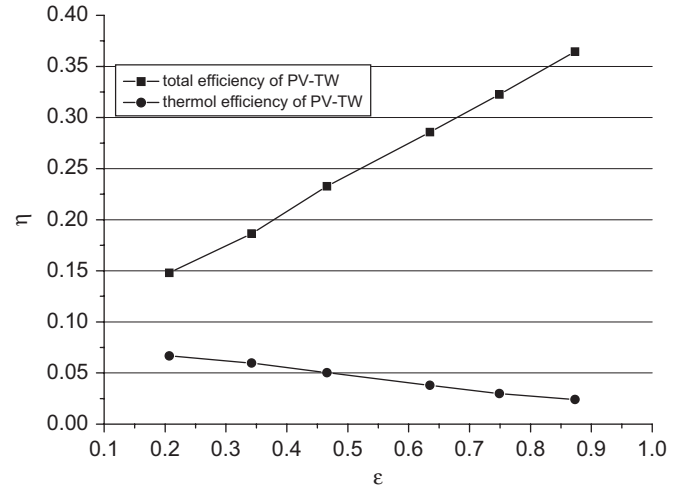


Fig. 10. The total efficiency and thermal efficiency of PV-TW in different coverage ratio.

TW is discussed, it is not the simple totaling of thermal energy and electrical energy. In Ref. [16], a total efficiency η_{total} , defined as follow, was given to evaluate the performance of PV/T system.

$$\eta_{total} = \eta_{th} + \eta_e / \eta_{power}, \quad (26)$$

$$\eta_{th} = \frac{Q_c + Q_k}{Q_s}. \quad (27)$$

We modified the total efficiency η_{total} as follows:

$$\eta_{total} = \eta_{th} + \eta_{e,sys} / \eta_{power}, \quad (28)$$

$$\eta_{e,sys} = \frac{E}{G}, \quad (29)$$

where Q_s is the solar radiation captured by the PV-glazing, η_{total} is the total efficiency of PV-TW system, η_{th} is the thermal efficiency of PV-TW system, η_e is the electrical efficiency of PV cells, $\eta_{e,sys}$ is the electrical efficiency of PV-TW system, η_{power} is the normal fuel electric plant efficiency, $\eta_{power} = 0.38$. As showed in Fig. 10, when the coverage ratio increases, the total efficiency of PV-TW increases and thermal efficiency of PV-TW decreases.

4. Conclusion

In this paper, a novel PV-TW is proposed. Based on the actual measured weather data in Hefei, a detailed simulation model for PV-TW is presented. The analysis of simulation results show that:

- The electrical efficiency of PV cells decreases when the coverage ratio increases. But in winter, the ambient temperature is quite low, hence the influence of coverage ratio on electrical efficiency is slight, less than 0.5%.
- As the coverage ratio increases, the electrical yield of PV-glazing increases, the air temperature in the air duct and the indoor temperature decrease. The maximum

indoor air temperature difference, corresponding to the lowest and the highest coverage ratio, can reach to 6.8 °C above. Therefore, in order to obtain a good adjustment of the indoor temperature, an appropriate coverage ratio should be chosen.

- As the coverage ratio increases, the total efficiency of PV-TW increases, but the thermal efficiency and the thermal heat gain through PV-TW decreases. So it is not the case that the larger area of PV cells brings the better thermal benefit.

Acknowledgement

The work described in this paper was sponsored by the National Science Foundation of China, Project number: 50408009.

References

- [1] Green MA, Zhao J, Wang A, Wenham SR. Process and outlook for high-efficiency crystalline silicon solar cells. *Sol Energy Mater Sol Cells* 2001;65:9–16.
- [2] Krauter S, et al. Combined photovoltaic and solar thermal system for facade integration and building insulation. *Sol Energy* 1996;67: 239–48.
- [3] Clarke JA, Hand JW, Johnstone CM, et al. Photovoltaic integrated building facades. *Renewable Energy* 1996;8:475–9.
- [4] Awbi H, Gan G. Simulation of solar induced ventilation. In: *Proceedings of CFD on environmental and building servers engineer*. Institute of Mechanical Engineers, London; 1991.
- [5] Haalannnd SE. Simple and explicit formulas for the friction factor in turbulent pipe flow. *J Fluid Eng* 1983;105:89–90.
- [6] Schweiger H, Soria M, Oliva A, Costa M. A software for the numerical simulation of glazed façade with ventilation channels, Basel word CFD. In: *Proceedings of third conference in applied computational fluid dynamics*, Freiburg I. Br.; 1996.
- [7] Van Schijndel AWM, Schol SFC. Modeling pressure equalization in cavities. *J Wind Eng Ind Aerodyn* 1998;74–76:641–9.
- [8] Mei L, Infield D, et al. Thermal modeling of a building with an integrated ventilated PV façade. *Energy Build* 2003;35: 605–17.
- [9] Smolec W, Thomas A. Some aspects of Trombe wall heat transfer models. *Energy Convers Manage* 1991;32:269–77.
- [10] Chen DT, Chaturvedi SK, Mohieldin TO. An approximate method for calculating laminar natural convective motion in a Trombe-wall channel. *Energy* 1994;19:259–68.
- [11] Gan, Guohui. A parametric study of Trombe walls for passive cooling of buildings. *Energy Build* 1998;27:37–43.
- [12] Brinkworth BJ, Cross BM, Marshall RH, Yang H. Thermal regulation of photovoltaic cladding. *Sol Energy* 1997;61:169–78.
- [13] Yang HX, Marshall RH, Brinkwoorth BJ. Validated simulation for thermal regulation of photovoltaic wall structures. In: *Proceedings of the 25th photovoltaic specialist conference, USA; 1996*.
- [14] Zondag HA, et al. The thermal and electrical yield of a PV-thermal collector. *Sol Energy* 2002;72:113–28.
- [15] Duffie JA, Beckman WA. *Solar engineering of thermal processes*. 2nd ed. New York: Wiley; 1991.
- [16] Huang BJ, et al. Performance evaluation of solar photovoltaic/thermal systems. *Sol Energy* 2001;70:443–8.